Ultrafast dynamics in van der Waals heterostructures

Chenhao Jin[1], Eric Yue Ma[2], Ouri Karni[2], Emma C. Regan[1,3,4], Feng Wang[1,4,5]*, Tony F. Heinz[2,6]*

[1] Department of Physics, University of California at Berkeley, Berkeley, California 94720, USA.
[2] Department of Applied Physics, Stanford University, Stanford, California 94305, USA.
[3] Graduate Group in Applied Science and Technology, University of California at Berkeley, Berkeley, California 94720, USA
[4] Material Science Division, Lawrence Berkeley National Laboratory, Berkeley, California 94720, USA.
[5] Kavli Energy NanoSciences Institute at University of California Berkeley and Lawrence Berkeley National Laboratory, Berkeley, California 94720, USA.
[6] SLAC National Accelerator Laboratory, 2575 Sand Hill Road, Menlo Park, California 94025, USA.

* Correspondence to: tony.heinz@stanford.edu, fengwang76@berkeley.edu

Abstract

Van der Waals heterostructures are synthetic quantum materials composed of stacks of atomically thin two-dimensional (2D) layers. Because the electrons in the atomically thin 2D layers are exposed to layer-layer coupling, the properties of van der Waals heterostructures are defined not only by the constituent monolayers, but also by the interactions between the layers. Many fascinating electrical, optical, and magnetic properties have recently been reported in different types of van der Waals heterostructures. In this review we focus on unique excited-state dynamics in transition metal dichalcogenide (TMDC) heterostructures. TMDC monolayers are the most widely studied 2D semiconductors, featuring prominent exciton states and accessibility to the valley degree of freedom. Many TMDC heterostructures are characterized by a staggered band alignment. This band alignment has profound effects on the evolution of the excited states in heterostructures, including ultrafast charge transfer between the layers, the formation of interlayer excitons, and the existence of long-lived spin and valley polarization in resident carriers. Here we review recent experimental and theoretical efforts to elucidate electron dynamics in TMDC heterostructures, extending from time scales of femtoseconds to microseconds, and comment on the relevance of these effects for potential applications in optoelectronic and valleytronic/spintronic devices.

Main text

Advances in the isolation and manipulation of atomically-thin sheets of two-dimensional (2D) crystals, starting with the investigations of graphene a decade ago, have ushered in a new era of basic scientific research and technological innovation. 2D layers with diverse properties can now be prepared separately and then stacked together to form new types of quantum materials, known as van der Waals (vdW) heterostructures. The ability to combine materials with monolayer precision enables the design and creation of functional 2D materials that do not exist in nature. Today we have at our disposal a wide variety of atomically thin 2D layers, ranging from semiconducting MoS_2 and insulating hexagonal boron-nitride (h-BN) to magnetic CrI_3 and superconducting $NbSe_2$, that can be stacked one upon the other. Since the electrons in atomically thin layers are exposed, different quantum states found in the individual layers can interact and couple to one another in ways that are not possible in other systems.

VdW heterostructures constitute a vast family of new quantum materials, since they are defined not only by the combination of constituent monolayer materials, but also by the stacking sequence and relative crystallographic alignment of the layers. Further control of physical properties in 2D vdW heterostructures can be achieved through the application of electrostatic gating and fields, as well as substrate and strain engineering. Many fascinating physical phenomena have been reported in different vdW heterostructures, as exemplified by transport measurements revealing Hofstadter butterfly states, fractional Chern insulators, gate-tunable Mott insulators, unconventional superconductivity, etc[1-7]. In addition to electrical transport, there has also been great progress in the study of the optical properties and excited-state dynamics in vdW heterostructures. Here we review the new dynamical phenomena that emerge in semiconducting vdW heterostructures composed of stacked transition metal dichalcogenide (TMDC) layers. We focus our discussion on TMDC heterostructures, since the individual TMDC layers, with their many distinctive and intriguing properties, have already been well characterized and provide a strong basis for understanding the emergent new properties of heterostructures.

TMDC semiconductors (MX_2 layers with 2H symmetry and M = Mo, W; X = S, Se, Te) exhibit direct gaps at monolayer thickness. They feature strong light-matter interactions and dramatically enhanced electron-electron interactions, with the optical properties largely defined by exciton states. The exciton binding energies in monolayer TMDCs are hundreds of meV– as much as two orders of magnitude larger than in typical bulk semiconductors like silicon or GaAs[8,9]. In addition, TMDC monolayers provide a platform to investigate and control the valley degree of freedom — often designated as valley pseudospin — associated with the energetically degenerate K and K' valleys and accessible optically through the presence of valley circular dichroism. The valley pseudospin in TMDC is, moreover, coupled to the electron/hole spin due to strong spin-orbit interactions[10,11].

Understanding the dynamic interplay and evolution of the charge, spin, and valley excitations in vdW heterostructures is of fundamental scientific interest. It is also of central importance for many potential applications of TMDC materials in optoelectronics, spintronics, and valleytronics. The dissociation of optically excited excitons into free carriers is, for example, critical for photovoltaic devices, while the ability to control and stabilize valley polarization is essential for valleytronic applications. The formation of vdW heterostructures in TMDC layers can profoundly affect their excited-state dynamics, ranging from the dissociation of intralayer excitons and the formation of interlayer excitons to the relaxation of spin and valley polarization. The use of vdW heterostructures provides a powerful platform to control and optimize the dynamic response of the constituent materials. In this review, we

survey recent progress in probing electron dynamics, extending from femtoseconds to microseconds, in TMDC heterostructures. On short time scales ($\lesssim$1ps), the dynamics is dominated by the charge transfer and energy relaxation processes in the heterostructure. On longer time scales ($\gtrsim$1ps), the recombination of interlayer excitons and relaxation of the spin and valley degrees of freedom become relevant. The rate of these processes can vary by orders of magnitude depending on the configuration, temperature, and doping of the heterostructure. We will also touch upon the dynamics of lateral transport of spin and valley polarization in TMDC heterostructures. We describe the physical mechanisms that underlie the different types of dynamic response in TMDC heterostructures and distinguish the behavior from that of the constituent layers, as well as mention briefly the implications for potential new technologies.

Band alignment in TMDC heterostructures

In describing the single-particle electronic states in a vertical TMDC heterostructure, most authors in the literature consider the states to be largely localized within the individual layers. This approximation holds well for electronic states close to the band gap due to unusually weak interlayer coupling in TMDCs at the relevant K and K' points in the Brillouin zone (Fig. 1a)[12]. Therefore one can directly examine the relative energy difference, or band alignment, of material-specific electronic band extrema, just as is commonly done for heterostructures and quantum wells based on bulk materials[13,14]. An important distinction for atomically thin layers is that the concept of band bending near an interface does not apply[15].

Semiconductor heterostructures can have different types of band alignment depending on the energy difference of the conduction and valence band extrema in the constituent layers (Fig. 1b) [13,14]: The lowest-lying states for electrons and holes reside in the same layer for a type-I heterostructure[16], but are separated in different layers for a type-II heterostructure[13,17]. Further offsets in energy could, in principle, lower the conduction band minimum (CBM) of one layer to a position below the valence band maximum (VBM) of the other layer, yielding a type-III heterostructure[18].

The type of band alignment has profound effects on the excited-state dynamics in a vdW heterostructure. In a type-I heterostructure carriers can only flow from the layer with the larger band gap to the layer with the smaller band gap (assuming that they do not have excess energy greater than the band offsets). The same applies to energy transfer through the exchange of virtual photons. In a type-II heterostructure, on the other hand, electrons accumulate in the layer with the lower CBM, while holes accumulate in the other layer[17,19,20]. Energy transfer can, however, still occur from the larger-gap to the smaller-gap material[21].

There have been numerous theoretical studies of the band alignment in TMDC heterostructures[13,14,18,22-24]. The result of one recent calculation is shown in Fig. 1c. Many of the theoretical studies make use of DFT or related methods and cannot accurately account for the effects of doping (Fermi level difference), dielectric screening, and excitonic interactions[25]. They provide nonetheless guidelines for realizing specific types of heterostructures and combination of band gaps. Although theoretical studies are advancing rapidly, at present a definitive determination of heterostructure band alignment must rely on experiment[26,27].

In the following, we describe experimental findings concerning the dynamics of charge and energy transfer for representative TMDC heterostructures, followed by a summary of the relevant theoretical studies.

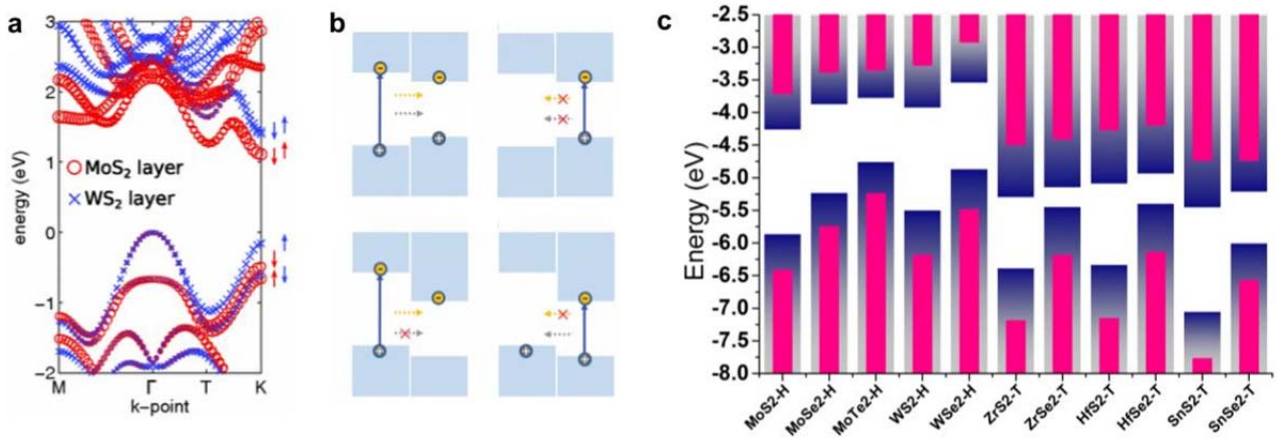

Fig. 1 Band alignment in vertical vdW heterostructures of TMDCs. (a) Calculated electronic states in a MoS_2/WS_2 vertical heterostructure, showing layer-localized states near the band edges at the K point[12]. (b) Schematic of allowed charge transfer in heterostructures with type-I (top) and type-II (bottom) band alignment[16]. (c) Calculated band-edge energies for various TMDCs[22] based on different theoretical treatments: DFT-PBE (blue) and G_0W_0 (pink).

Charge transfer and energy transfer in TMDC heterostructures - Experiment

Following the predictions of type-II band alignment in TMDC heterostructures, several experimental studies were reported that aimed (among other goals) to validate these theoretical results by probing the associated charge transfer (CT) or energy transfer (ET) processes. Vertical heterostructures have been examined for various material combinations prepared with different fabrication methods, including stacking of layers exfoliated from bulk crystals and from layers grown by chemical vapor deposition (CVD), as well as heterostructures grown directly by CVD.

Ultrafast optical measurements using pump-probe spectroscopy provide the possibility of accessing charge and energy transfer processes with femtosecond (fs) time resolution. In initial experiments, Hong *et al*. examined the dynamics of the MoS_2/WS_2 heterostructure. Following excitation by an ultrafast laser pulse resonant with the lower-energy MoS_2 A exciton, they observed a transient change in reflectivity near the *higher-energy* WS_2 exciton (Fig. 2a)[19]. Based on theoretical predictions of type-II band alignment of the two materials, this transient response was identified as arising from CT of a hole from the MoS_2 monolayer to the WS_2 monolayer. By deconvolving the instrument response from the rise-time of the signal, the authors were able to provide an upper limit of 50 fs for the charge transfer time. Ceballos *et al.* observed similar dynamics in a heterostructure of $MoS_2/MoSe_2$, without spectrally resolving the reflection of the probe[28]. They concluded, based on the theoretically predicted band alignment, that electrons were transferred from $MoSe_2$ to MoS_2. In addition, when exciting both layers (using excitation resonant with the higher-energy exciton feature in MoS_2) and comparing the

transient reflectivity signal of the monolayers to that of the heterostructure, the authors identified the presence of hole transfer in the opposite direction, *i.e*., from MoS_2 to $MoSe_2$ (Fig. 2b).

Following these first experimental investigations, several groups examined the nature of the ultrafast CT for different types of heterostructures under different conditions. Heo *et al.* compared CVD-grown and manually stacked WS_2/MoS_2 heterostructures with a focus on the dependence on the relative (twist) angle of the two constituent lattices[29]. Measuring the transient transmission of the probe signal, they did not resolve differences in the rise time of the signal associated with CT, but did observe a pronounced difference in the decay times of the signal. Wang *et al.* examined several WSe_2/WS_2 heterostructures composed of CVD-grown layers mechanically stacked with different twist angles[20,29]. Using pump-probe measurements, together with steady-state techniques such as reflection contrast spectroscopy, they showed the same ultrafast signature from the onset of CT, either from electrons moving from WSe_2 to WS_2 or from holes traveling in the opposite direction. They concluded that interlayer CT takes place within 450 fs, close to the duration of the pump pulses in their experiment, and does not exhibit measurable sensitivity to the twist angle. Further reinforcing this conclusion, Zhu *et al*. explored deterministically aligned heterostructures of mechanically exfoliated MoS_2 and WSe_2; they that the CT signal appears within 40 fs regardless of twist angle (Fig. 2c)[30]. On the other hand, the time scale of the decay was varied with the twist angle, but without any clear trend. Ji *et al.* reported a similar CT rise time for stacks of CVD-grown MoS_2 and WS_2 (Ref [31]). Such rapid interlayer CT irrespective of crystal orientation (and thus crystal momentum) is somewhat unintuitive. Chen *et al*. probed intraband transitions in a heterostructure using infrared light and suggested a potential explanation based on the rapid formation of “hot” interlayer excitons[32]. Additional theoretical investigations are summarized in the next section.

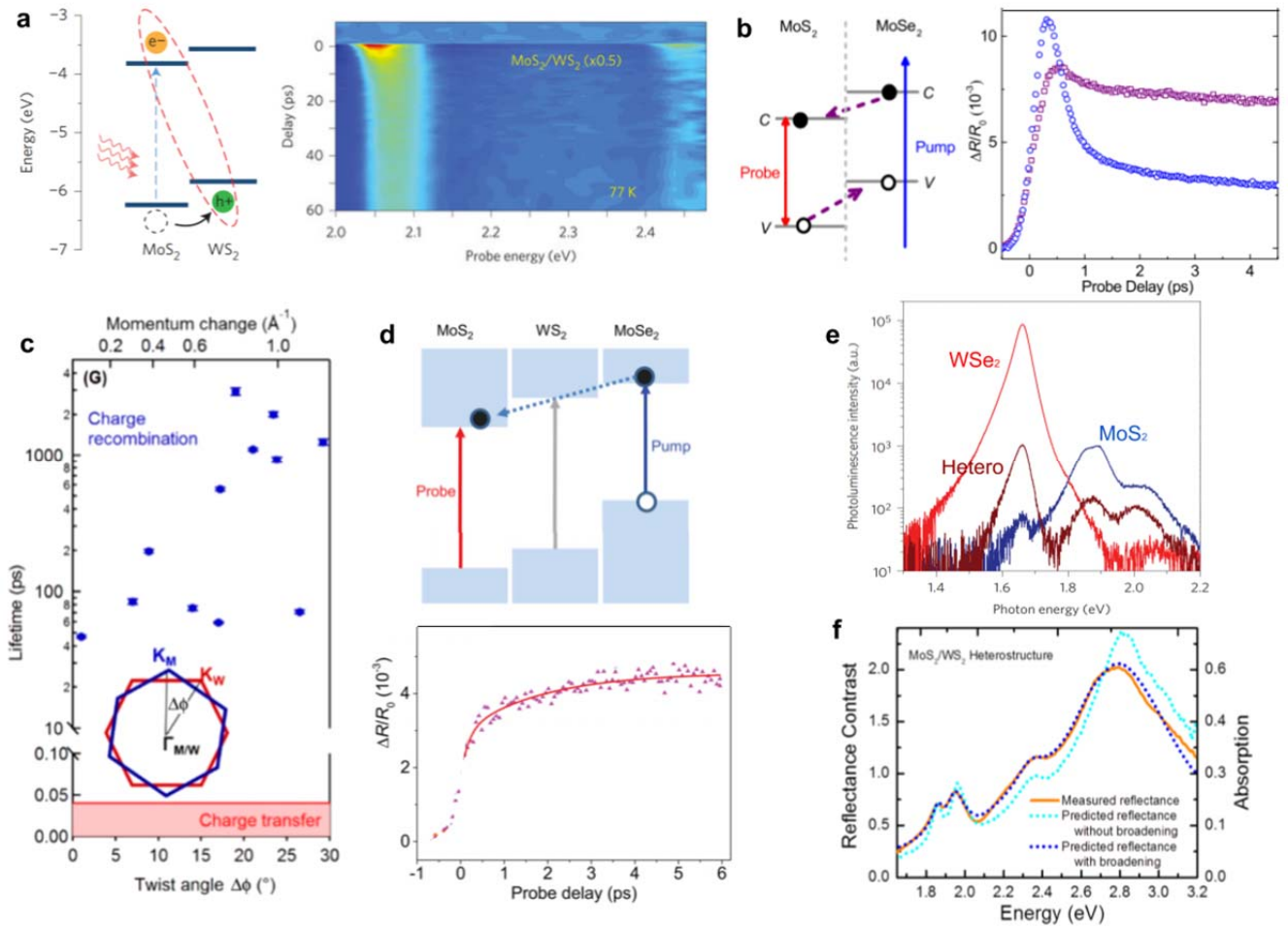

Fig. 2 Experimental studies of ultrafast charge transfer in vertical TMDC heterostructures. (a) Schematic and energy-resolved transient absorption spectra of a MoS_2/WS_2 heterostructure, excited by an optical pulse near the lower-energy MoS_2 A exciton feature, indicating hole transfer[19]. (b) Schematic and time-resolved differential reflection of a $MoS_2/MoSe_2$ heterostructure (blue) and of monolayer MoS_2 (purple), excited by an optical pulse above the band gaps of both materials, indicating both electron and hole transfer[28]. (c) Charge transfer (red shading) and recombination (blue) times in heterostructures of MoS_2 and WSe_2 with different twist angles, as indicated[30]. (d) Differential reflection at the energy of the MoS_2 A exciton following excitation at the energy of the $MoSe_2$ A exciton in a $MoSe_2/WS_2/MoS_2$ trilayer heterostructure[33]. (e) PL quenching[34] in MoS_2/WSe_2 and (f) broadening of the features absorption features[35] in a MoS_2/WS_2 heterostructure compared to the response of the separated monolayers.

Further demonstrating its robustness, the signature of ~ps electron transfer was observed in a trilayer heterostructure where monolayers of $MoSe_2$ and MoS_2 were separated by a monolayer WS_2 (Fig. 2d, Ref [33]). The authors suggested that such rapid CT across multiple materials is coherent, rather than sequential.

CT dynamics was also revealed in investigations of the coupling between pairs of TMDC layers. CT in a $MoS_2/MoTe_2$ heterostructure was identified using pump-probe experiments[36], leading to the suggestion of $MoTe_2$ as a good electrical contact for other semiconducting TMDCs and metals. Later, cascaded transfer of electrons and holes across several TMDCs heterostructures was invoked to explain correlated blinking observed in the photoluminescence (PL) in those stacks[37].

In addition to these time-resolved pump-probe measurements, CT between two TMDC layers in a heterostructure has been inferred from quenching of the photoluminescence of the constituent monolayers[19,20,28-33,38-40] and by broadening of the resonant features in the monolayers in optical absorption measurements[20,35], both phenomena arising as a consequence of the presence of additional relaxation channels in the heterostructures. A reduction in the PL intensity by factor of a few tens to a few hundreds has commonly been observed (Fig. 2e)[19,34]. This suggests a corresponding ratio for the charge transfer time compared to the population lifetime in the isolated material. Assuming the latter to be a few hundred picoseconds for excitons in monolayer TMDCs[41] at room temperature, we estimate a CT time of ~1 ps, somewhat longer than measured by pump-probe techniques. This discrepancy can be explained as the result of a small fraction of the heterostructure exhibiting poor contact between the layers, thus yielding reduced PL quenching compared to that of the ideal structure. In optical absorption measurements, linewidth broadening of heterostructures compared with that of the separate monolayers has been reported and used to estimate non-radiative decay rates comparable to those deduced from pump-probe experiments (Fig. 2f)[35]. Extrinsic factors, such as strain introduced in fabricating the heterostructure, can potentially also play a role. The extremely rapid (few femtosecond) relaxation times inferred for high-lying states may, however, remain difficult to probe directly in the time domain, but is easily observable by lineshape analysis.

Another dynamic process that may compete with CT is energy transfer (ET). In this latter process, an exciton created in one layer recombines, and the released energy creates an exciton in the other layer. Kozawa *et al.* reported evidence for such a process in a $MoSe_2/WS_2$ heterostructure (Ref [21]) on the basis of a measured enhancement of PL from the $MoSe_2$ feature under excitation resonant with the WS_2 optical band gap. Recently, ET was also identified in heterostructures of MoS_2 and WS_2 separated by insulating layers of h-BN[42]. In these structures, PL quenching from the heterostructure was reduced, or even become PL enhancement, upon increasing the thickness of the h-BN spacer. This was interpreted as an ET process between B excitons in MoS_2 and A excitons in WS_2. The dependence of the enhancement on spacer thickness, with an optimum of PL enhancement for ~5 layers of h-BN and subsequent reduction of this effect with increasing layer thickness, is compatible with the predicted trend for a dipole-dipole interaction. This highlights the major difference between ET and CT processes: While the latter requires intimate coupling of the two constituent monolayers, the former, originating in dipole-dipole interactions, can act at greater distances and across insulating spacers. Although this difference between the processes is clear, there is currently little direct experimental information on the absolute rates of energy transfer for TMDC layers and in what regimes and under what conditions energy transfer competes with charge transfer.

Charge transfer and energy transfer in TMDC heterostructures – Interpretation and theory

Since most experiments have excited and probed excitonic resonances of the constituent layers, it has often been assumed that CT occurs between their direct band-edge (K/K' valley) states. Band structure calculations have shown that the K/K' states are localized around the central layer of metal atoms and have weak interlayer interactions. On the other hand, for states of different momentum,

such as in the Γ or Q valleys, the interlayer coupling may be significantly stronger. One consequence of this difference is the transition from indirect to direct band gap upon thinning TMDCs to the monolayer limit: the bulk CBM in the Q valley, more affected by interlayer coupling, lies above the K valley in monolayers[43,44]. For the same reason, the K-valley states are not expected to show such rapid interlayer charge transfer. This contradiction with experiment is further heightened by the apparent independence of CT on twist angle and lattice mismatch, the factors that dictate the momentum difference between the initial and final states, as well as its insensitivity to temperature. Here we briefly survey some of the approaches presented in the literature to identify the mechanism responsible for the very efficient CT processes observed experimentally in vertical TMDC heterostructures.

Zhu *et al*., following considerations relevant for CT processes in molecular systems, have pointed out the possible role of localization in bridging the momentum mismatch[45]. The electrostatic attraction between the optically excited electron and hole, which leads to the formation of tightly bound excitons, gives rise to a distribution of momenta for the charge carriers across a significant range wavevectors in the Brillouin zone (BZ). This situation could explain the apparent lack of momentum conservation in the observed CT process. However, it is unclear with this effect alone could supply the large momentum required for CT in heterostructures with large twist angles[30]. In addition, for excitation substantially above the band gap, it is unclear whether exciton formation occurs prior to charge transfer[28].

Several groups have also employed numerical calculations using molecular dynamics (MD) and time-dependent density-functional theory (TD-DFT) to elucidate the mechanism for interlayer charge transfer. Since accurately accounting for the effect of excitons is computationally demanding, these calculations have focused on the transfer of free charge carriers from one monolayer to its neighbor. Wang *et al.* described a process of transferring holes directly between the K valleys of the two layers mediated by the electric dipole interaction of the initial and final states, which enhances the coupling between the states to above a critical level for collective charge transfer[46]. In this description, both twist angle and temperature have a significant influence on the transfer rate[46]. Zhang *et al.* pointed out the significance of such dipole coupling between specific states in the vicinity of the K valley and highlighted the expected twist-angle dependence of the CT rate[47]. Additionally, the authors argue that the omission of excitonic effects for above gap excitation may not be significant if the time scales for CT and exciton formation are comparable. (This argument is, however, problematic for explaining CT from excitons created directly by resonant excitation.)

A slightly different picture is presented by Long *et al*.[48] and by Li *et al*.[49] for CT processes in $MoSe_2/MoS_2$ and MoS_2/WS_2 systems, respectively. They propose that holes and/or electrons undergo transfer from one layer to the other due to mixing between the electronic states near the K point of both layers[48,49]: the states into which the charge carriers are optically injected are coherently mixed (and therefore delocalized) across the two layers, so that CT need only to be driven by an intralayer relaxation process to the K-valley, mediated by phonon emission. In this model, the coupling relies on specific layer orientations to facilitate the state mixing in the heterostructure. The discrepancy between this requirement and the apparent twist-angle independence of CT in experiments is explained in terms of changes in the relative local atomic positions in the two layers across the moiré pattern of the heterostructure[50,51]. Regardless of the twist angle of the layers, such lateral inhomogeneity provides regions where the coupling between the layers is strong[31]. In all of the above scenarios, phonons are necessary for the completion of the CT process, but not for its initiation.

Recent work has also explored a more direct role for phonons in the initiation of CT. Wang *et al.* considered momentum-conserving charge transfer between the layers in various regions of the BZ, including at the K, Q and Γ points for different twist angles and degrees of lattice mismatch[52], as shown in Fig. 3a-d. The proposed mechanism involves scattering by phonons from the K valley to the Γ valley (for holes) or to the Q valley (for electrons), regions where the interlayer coupling is strong and interlayer charge transfer is rapid. After charge transfer, scattering with another phonon would bring the charge carriers back to the K-valley. For intralayer scattering within 20 fs, the entire charge transfer process would occur in less than 100 fs, as observed experimentally. A similar scheme was developed by Zheng *et al.* using a numerical MD TD-DFT calculation, although without accounting for inhomogeneities from the moiré pattern[53]. These theories better match the observed twist-angle independence, as the coupling around the Γ and Q points is not sensitive to the layer orientation. The expected temperature dependence of this mechanism is also weak, as it only requires emission of phonons to dissipate the excess energy available from the transfer. This general mechanism has been adopted in the interpretation of recent experiments related to CT processes[30,33,39].

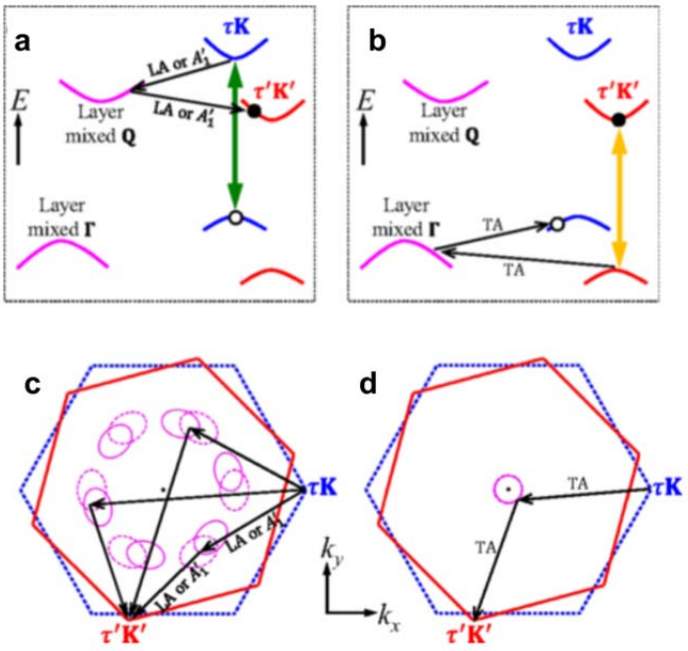

Fig. 3 Theoretical concepts explaining the robust and ultrafast nature of CT in TMDC heterostructures[52]. (a) Schematic representation of phonon mediated electron transfer. (b) The same for hole transfer. (c) Top view of the twisted BZ of the two layers, where electron transfer between the K-points is mediated by phonon coupling to the Q-point. (d) The same for hole transfer, mediated in this case by the coupling to the Γ-point.

Spin and valley dynamics in TMDC heterostructures

The previous sections addressed carrier dynamics in TMDC heterostructures on the ultrafast time scale ($\lesssim$1ps) relevant for interlayer charge transfer in systems with type-II band alignment. In the following section, we focus on spin and valley relaxation dynamics in TMDC heterostructures, which take place on considerably longer time scales.

Within a TMDC monolayer, there are two distinct relaxation processes to consider. First, the population decay of optically excited excitons has a characteristic time scale of few picoseconds to nanoseconds, depending on choice of material, sample preparation, temperature, etc.[54-58]. Second, the exciton spin-valley lifetime, which determines how long information can be stored in the spin-valley degree of freedom, has been found to be a few picoseconds in isolated monolayer TMDCs[59-63]. Both the population and the spin-valley lifetimes in type-II heterostructures, where the electrons and holes reside in different layers after the rapid initial charge transfer process, can differ markedly from the corresponding lifetimes in isolated monolayers.

Below we review recent experimental results on dynamics on the pico-to-micro-second time scale in heterostructures and show that both the population lifetime and the spin-valley lifetime can be significantly longer than for the monolayer case. We then summarize recent efforts towards understanding the physical mechanisms of the corresponding intervalley scattering processes. Finally, we discuss the spatio-temporal dynamics of spin and valley polarization in TMDC heterostructures.

Long spin and valley lifetime in TMDC heterostructures

Traditional electronic devices are based on the manipulation of electron charges in the real space. Using other electron degrees of freedom as the information carrier, such as spin and valley, can potentially overcome fundamental limits of speed and power consumption, giving rise to intriguing new concepts in spintronics and valleytronics. A long spin/valley lifetime is necessary to ensure that the spin/valley information will be maintained in the idle state and can persist long enough to be processed. We note that the valley lifetime discussed here should not be confused with the valley depolarization time: the former can originate from different mechanisms, including the population decay of the valley information carriers, while the latter only describes the intervalley scattering process.

TMDCs offer a promising platform for spintronic and valleytronic applications, owing to several attractive properties of these materials. The valley-dependent optical selection rule allows for convenient creation, manipulation, and detection of excitons in specific valleys with circularly polarized light[64-66]. Furthermore, the spin-valley locking effect suggests that a very long spin-valley lifetime is possible because intervalley scattering of electrons or holes requires both a large momentum change from K to K' and a simultaneous spin flip[10,11]. However, several groups have measured exciton spin-valley dynamics using time-resolved Kerr rotation (TRKR)[59-63], and the spin-valley lifetime was found to be rather short, ranging from one to few picoseconds, even at low temperatures. This counter-intuitive observation was later explained as a consequence of the exchange interaction between excitons in the two valleys[67-70]: a bright exciton always has total momentum and spin of zero and therefore does not require any change in momentum or spin to scatter to the other valley as an intact exciton. This reduced spin-valley lifetime of excitons in TMDC monolayers significantly limits their use in carrying spin-valley information.

A general strategy for improving the spin-valley lifetime in TMDCs is to eliminate the exciton exchange interaction by converting excitons into other excitations that serve as alternative carriers of valley information. An additional figure of merit, the conversion efficiency, must be introduced to quantify the final valley imbalance created from each optically excited exciton. To avoid loss of valley information during conversion, the time scale of the conversion process (*i.e*., the exciton population lifetime) must be comparable to or shorter than the picosecond spin-valley lifetime of excitons. In monolayer TMDCs, several candidates have been considered as the alternative information carriers, including trions[71-73], dark excitons[74,75], biexcitons[76,77], and resident carriers[78-81]. For example, Fig. 4a,b show the valley dynamics of trions and resident electrons probed by TRKR measurement. Unlike bright excitons, these excitations have non-zero total momentum and/or total spin, and therefore will not suffer from rapid spin-valley relaxation through the exchange interaction. Their spin-valley lifetimes at low temperatures range from tens of picoseconds to a microseconds, but the conversion efficiency from the initially generated exciton has rarely been characterized. However, since the exciton population lifetime is comparable to or longer than the exciton spin-valley lifetime in these cases, the valley conversion efficiency is likely to be considerably less than unity.

On the other hand, the interlayer charge transfer process in type-II heterostructures provides an attractive mechanism to break intralayer excitons on the femtosecond time scale. As discussed above, the ultrafast charge transfer process occurs very rapidly, typically within ~50 fs, in TMDC heterostructures[19,82]. Because this time scale is much faster than exciton spin-valley relaxation, the loss of spin-valley information during the conversion process is expected to be minor.

In nearly aligned heterobilayers, electrons and holes can form bright interlayer excitons after the charge transfer process[28,40,83]. Rivera *et al*. observed 40% positive circular helicity from interlayer exciton emission in $WSe_2/MoSe_2$ bilayer and measured a spin-valley lifetime of a few nanoseconds in a time-resolved photoluminescence (TR-PL) study[84], as shown in Fig. 4c. The significantly longer spin-valley lifetime of interlayer excitons can be understood by noting that the electron and hole wavefunctions have much smaller overlap in interlayer excitons compared to intralayer excitons; they will therefore have a weaker exchange interaction and exhibit slower recombination processes (both radiative and non-radiative).

Recently, there has been increasing research interest in the nature of the interlayer exciton state and the origin of the circular helicity of emission in nearly aligned heterostructures. Hsu *et al*. reported negative circular helicity of interlayer exciton emission[85] in $WSe_2/MoSe_2$ bilayer, while Ciarrocchi *et al*. and Hanbicki *et al*. observed two separate interlayer exciton emission peaks with opposite signs of helicity[86,87]. Meanwhile, various configurations of interlayer excitons have been proposed as the emitting state, including spin singlet zero-momentum excitons[84,88], spin-triplet zero-momentum excitons[89], and finite-momentum excitons[90,91]. The rich set of observations originates in part from the complex conduction band structure in the $WSe_2/MoSe_2$ bilayer, where electron states of spin up and spin down, and at K and Q valleys, are all close in energy. Furthermore, the real-space distribution of interlayer excitons when a moiré pattern is present can further modify the optical selection rules [92,93]. The exact mechanisms behind these interesting observations are yet to be fully understood.

An alternative approach involves using single-particle states, such as holes in WSe_2 to carry valley information in the heterostructure. Because the momentum match between electrons and holes (required for efficient exciton emission) is not relevant in this approach, a large-twist-angle bilayer is

preferred to separate electrons and holes in momentum space and further reduce their exchange interaction and recombination rate. Kim *et al.* measured the spin-valley lifetime of holes in WSe_2/MoS_2 heterostructures using circularly polarized pump-probe spectroscopy[94]. Figure 4d shows the measured decay dynamics of the total hole population and valley-polarized hole population in the WSe_2 layer at a temperature of 10 K. Both the population lifetime and the spin-valley lifetime of holes are around one microsecond, indicating that the decay of the spin-valley imbalance occurs primarily through population loss. On the other hand, the valley polarization remains almost a constant for a few microseconds, from which one can extract a valley depolarization time (or intervalley scattering time) exceeding 40 μs. The other critical figure of merit, the conversion efficiency, was also determined experimentally to be close to unity for valley-polarized holes[94]. The nearly ideal conversion efficiency is consistent with an interlayer charge transfer process that is far faster than intervalley scattering processes.

The spin-valley lifetime of resident holes in the heterostructure can be further improved by tuning the carrier concentration. Figure 4e summarizes the doping-dependent spin-valley lifetime of holes in a WSe_2/WS_2 heterostructure (red circles), as compared to the population lifetime of holes (blue triangles)[95]. In charge neutral and electron-doped heterostructures, the spin-valley lifetime is similar to the population lifetime; however, for hole-doping, the spin-valley lifetime becomes orders of magnitude longer than the population lifetime. This doping dependence is a consequence of the interlayer electron-hole recombination process, as shown in Fig. 4f,g. For electron-doped or charge neutral heterostructures (Fig. 4f), all of the holes in WSe_2 are pump-generated excess holes. Therefore, when hole population decays to zero due to interlayer electron-hole recombination, no holes -- and certainly no valley-polarized holes -- remain in the WSe_2. The valley lifetime is then limited by the lifetime of the total hole excess. On the other hand, if the original hole density is much greater than the photo-generated density, excess electrons in WS_2 will recombine with holes from both valleys of WSe_2 with nearly equal probability (Fig. 4g). Consequently, a pure spin-valley imbalance (*i.e.*, equal excess and deficiency of holes in the K and K' valley) is generated, the lifetime of which can be much longer than the population lifetime and has been found to exceed 20 μs. Furthermore, the decrease of spin-valley imbalance is negligible during the population decay, and the overall efficiency of this two-step conversion process can approach 100%[95].

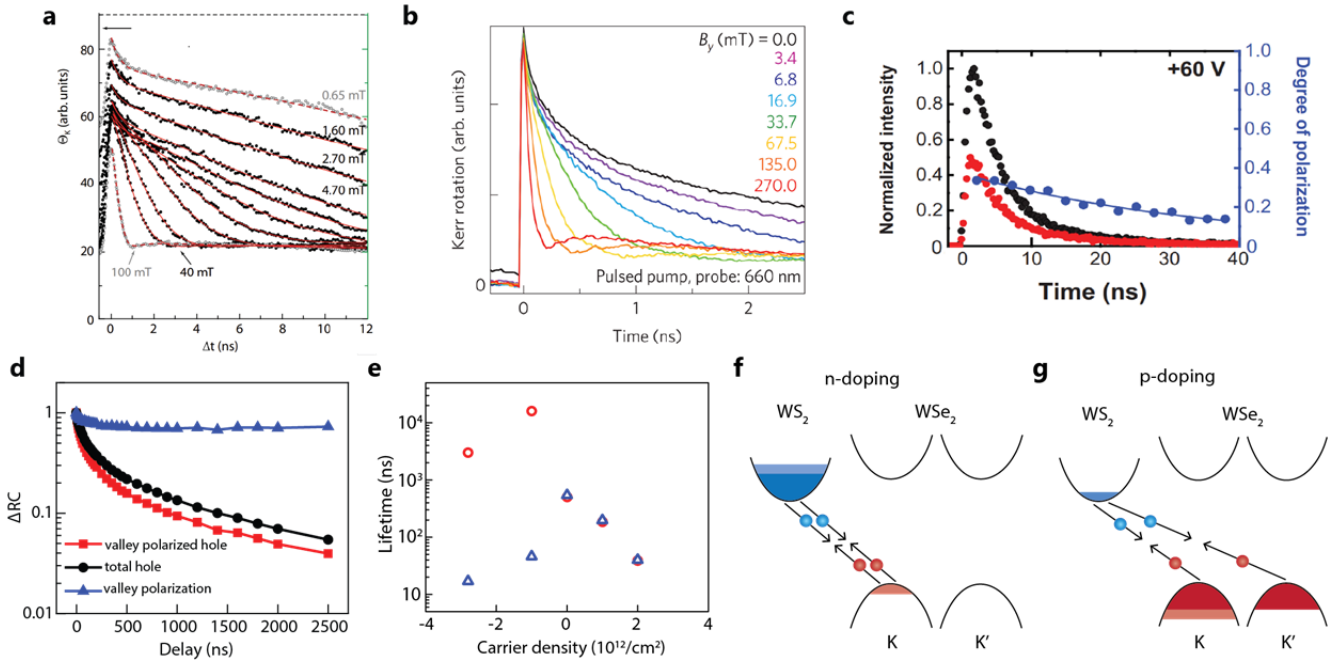

Fig. 4 **Dynamics of spin-valley information carriers in TMDC materials**. (a-b) Spin-valley dynamics of trions (a)[72] and resident electrons (b)[81] in monolayer TMDC materials under different external magnetic fields as probed by time-resolved Kerr rotation measurements. A spin-valley lifetime of few to tens of nanoseconds is observed at low fields. (c) Time-resolved photoluminescence in a nearly aligned $WSe_2/MoSe_2$ heterobilayer for the same (black) and opposite (red) circularly polarized excitation, revealing a valley lifetime of few nanoseconds[84]. (d) Decay dynamics of the valley-polarized hole population, the total hole population, and the valley polarization in a large-twist-angle WSe_2/MoS_2 heterostructure at charge neutrality[94]. (e) Summary of the hole population (blue) and spin-valley (red) lifetimes as a function of carrier concentration in a large-twist-angle WSe_2/WS_2 heterostructure[95]. (f-g) Schematic illustration of the interlayer electron-hole recombination process in electron-doped (f) and hole-doped (g) heterostructures.

Potential mechanism behind intervalley scattering

As discussed in the previous sections, the spin-valley lifetime can be limited either by the population lifetime or by the intervalley scattering process. The first limitation can be removed for valley-polarized holes in hole-doped heterostructures, making them promising candidates for spin-valley information carriers. Furthermore, directly probing hole dynamics provides relatively clean information about the decay mechanism owing to the simplicity of the valence band maximum. This configuration thus provides a valuable platform for understanding intervalley scattering processes in TMDC materials.

Figure 5a shows the decay dynamics of valley polarization at different temperature for holes in WSe_2/MoS_2 heterostructures, with the valley depolarization lifetime summarized in Fig. 5b (Ref. [94]).

The depolarization lifetime changes from 10 ns at 77 K to above 40 μs at 10 K, which roughly follows a thermally activated rate: $\tau \sim exp\left(\frac{\Delta}{k_B T}\right)$, with k_B denoting the Boltzmann constant and Δ ~ 20 meV.

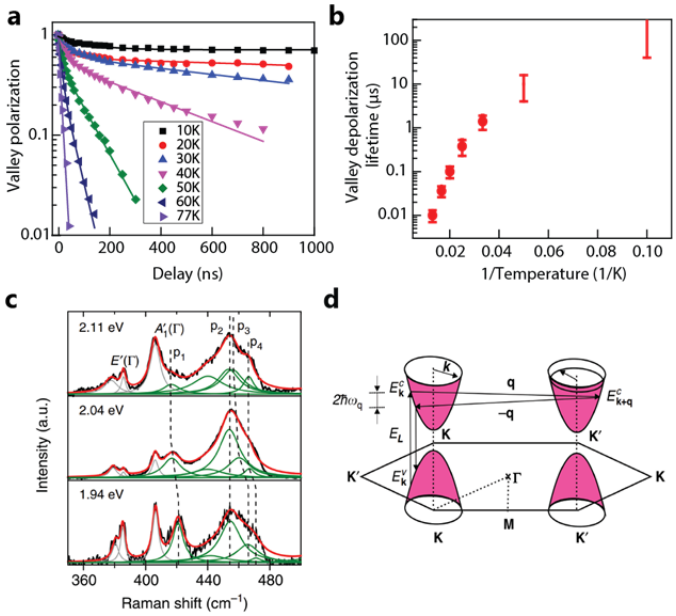

Fig. 5 **Potential origin of intervalley scattering in** WSe_2/MoS_2 heterostructures. (a) Temperature-dependent decay dynamics of valley polarization. (b) Temperature dependence of the intervalley scattering time. The process can be described as thermally activated[94]. (c) Resonant Raman spectra of single-layer MoS_2 show particularly strong second-order Raman signals (peaks p1 to p4) for excitation around 2.0 eV through a doubly resonant Raman (DRR) process involving K point phonons, as illustrated in (d)[96].

The inter-valley scattering of holes in WSe_2 requires a large momentum change and a simultaneous spin flip. However, due to the strong spin-orbit coupling in WSe_2, the picture of electrons and holes with perfectly defined up and down spin states in the K and K' valleys, respectively, is not strictly valid for states away from the K and K' points. Therefore, inter-valley scattering of carriers near, but not exactly at K and K' points is allowed. This process, often designated as the Elliott-Yafet mechanism, has a characteristic temperature dependence of

$$\tau_{EY}^{-1} \sim T^2 \, \tau_p^{-1},$$

where τ_p is the momentum scattering lifetime for a spin-conserving process. The T^2 -dependence originates from the fact that at higher temperature, thermally excited carriers are further away from band minima (K or K') and will therefore scatter more efficiently. However, the predicted T^2 dependence does not describe the strong observed variation with temperature, which presumably reflects from the temperature dependence of τ_p^{-1}. Indeed, a thermally activated temperature dependence is expected for phonon-assisted intervalley scattering at low temperatures, and the experimental activation energy of ~20 meV agrees with WSe_2 phonon energy (at the K-point) required for intervalley scattering[96]. Phonon-assisted intervalley scattering, accompanied by spin flip through the Elliott-Yafet mechanism, can thus account for the observed spin-valley depolarization of holes.

The important role of K-point phonons in intervalley scattering is also supported by a recent resonant Raman study[96], which reveals second-order Raman signals (peaks p1 to p4 in Fig. 5c) assigned to K-point phonons through a doubly resonant Raman (DRR) scattering process. This observation suggests a strong interaction between charge carriers and K-point phonons, which dramatically enhances their second-order Raman signals through the DRR process illustrated in Fig. 5d.

Spin-valley transport in TMDC heterostructures

The efficient generation of pure spin-valley imbalance in hole-doped WSe_2/WS_2 heterostructures provides a convenient way to create pure spin-valley current (Fig. 6a), which lies in the heart of spin-valley-tronic devices. Jin *et al*. performed space-and-time-resolved pump-probe spectroscopy to track the evolution of the spin-valley imbalance and to image the flow of pure spin-valley diffusion currents (Fig. 6b). Figure 6c shows experimental results for a hole-doped WS_2/WSe_2 heterostructure at an initial electrostatic hole doping of $p_0 = 1 \times 10^{12}\ /\mathrm{cm}^2$. At zero time delay, the spin-valley imbalance matches the pump beam spatial profile (half-width of ~1.5 $\mu\mathrm{m}$); the signal is negligible for a pump-probe separations greater than 3 $\mu\mathrm{m}$, as expected based on the convolution with probe spatial profile. At finite delay time, the spin-valley imbalance diffuses out of the excitation region, generating a pure spin-valley current. This leads to a strong decrease and increase of signal, respectively, in regions near and far away from the pump beam. The spin-valley current propagates to distances over 8 $\mu\mathrm{m}$ within 800 ns. Such direct imaging of the experimental spin-valley current flow (Fib. 6c) allows us to determine important physical parameters by comparison with a diffusion-decay model (Fig. 6d). We infer a diffusion constant of $D = 0.2\ \mathrm{cm}^2/\mathrm{s}$, a spin-valley lifetime of $\tau = 20\ \mu\mathrm{s}$, and deduce a spin-valley diffusion length of $l = \sqrt{D\tau} = 20\ \mu\mathrm{m}$.

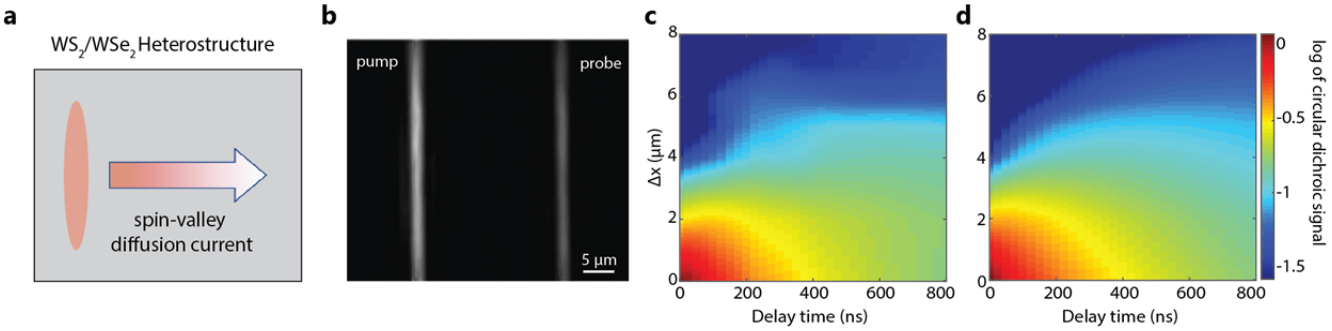

Fig. 6 **Spin-valley transport in a vdW heterostructure**[95]. (a) Optical excitation of pure spin-valley imbalance at the left edge of a device will create a pure spin-valley diffusion current flowing to the right without any associated charge current. (b) Experimental configuration for direct imaging of the spin-valley current flow with space-and-time resolved pump-probe spectroscopy using pump and probe beams focused to lines on the sample at defined spatial separation. (c-d) Experimentally measured spatio-temporal evolution of the pure valley imbalance in the heterostructure (c) and a simulation of the results using a diffusion-decay model (d) for an initial hole doping of $10^{12}/\mathrm{cm}^2$.

The efficient generation of spin-valley current with remarkably large current densities reflects the nearly ideal conversion of photogenerated excitons into a spin-valley imbalance. Still higher spin-

valley currents may be achievable in TMDC heterostructures by increasing the initial hole doping level to enable stronger optical pumping, as well as by improving the device quality to enhance the diffusivity. The long spin-valley lifetimes and diffusion lengths of valley-polarized holes in TDMC heterostructures hold promise for the generation, transport, and detection of spin-valley information and open exciting opportunities for the realization of future spintronic and valleytronic devices.

Concluding remarks

Despite the rapid progress in the study of excited-states in van der Waals heterostructures summarized above, many outstanding questions remain in understanding charge transfer processes and the spin and valley relaxation dynamics.

A complete picture of the underlying mechanism for the CT process in TMDC heterostructures remains elusive. First, the mechanisms developed to date do not account for the Coulombic interactions between electrons and holes, despite the existence of strongly bound excitons both in the TMDC monolayers[8,97,98] and in the heterostructures[40]. Though one can argue that the excitonic states are superpositions of the quasiparticle band states and, hence, are affected similarly, a quantitative picture in which excitonic correlations are taken into account remains a theoretical challenge. In this context, it would also be interesting to learn whether the dielectric environment of the heterostructure, which affects the excitonic interactions, also significantly influences the rate and efficiency of CT processes. In addition, the fact that changes in the dielectric screening of Coulombic interactions in TMDCs modify the quasiparticle band structure may provide a route to test the role of the Q and Γ valleys in CT processes. Second, the time-domain probes of CT to date have been limited in their by the instrumental response function and have not generally yielded precise CT times. In addition, optical measurements, with their limited spatial resolution, average over moiré patterns formed between the two layers. This may lead to a washing out of predicted trends for CT times. Overcoming these limitations by improved temporal resolution and/or spatial resolution (such as through near-field techniques) would provide important experimental information to inform and test further theoretical models.

Similarly many outstanding questions exist regarding spin and valley dynamics in TMDC heterostructures. Much more work is required to understand fully the intrinsic spin and valley dynamics in TMDC heterostructures and the dependence of the dynamics on the constituent TMDC materials, their relative crystallographic alignment, and their stacking order in multilayers. It remains, for example, unclear what factors define the ultimate limit for the spin-valley lifetime in TMDC heterostructures; also unknown is the role played by defects, edges, and grain boundaries, as well as possible effects from large-period moiré superlattices formed in TMDC heterostructures with small twist angles.

References

1 Hunt, B. *et al.* Massive Dirac Fermions and Hofstadter Butterfly in a van der Waals Heterostructure. *Science* **340**, 1427-1430, (2013).

2 Ponomarenko, L. A. *et al.* Cloning of Dirac fermions in graphene superlattices. *Nature* **497**, 594-597, (2013).

3 Dean, C. R. *et al.* Hofstadter's butterfly and the fractal quantum Hall effect in moire superlattices. *Nature* **497**, 598-602, (2013).

4 Spanton, E. M. *et al.* Observation of fractional Chern insulators in a van der Waals heterostructure. *Science* **360**, 62-66, (2018).

5 Cao, Y. *et al.* Unconventional superconductivity in magic-angle graphene superlattices. *Nature* **556**, 43-+, (2018).

6 Cao, Y. *et al.* Correlated insulator behaviour at half-filling in magic-angle graphene superlattices. *Nature* **556**, 80-+, (2018).

7 Chen, G. *et al.* Gate-Tunable Mott Insulator in Trilayer Graphene-Boron Nitride Moiré Superlattice. *Arxiv*, 1803.01985, (2018).

8 Chernikov, A. *et al.* Exciton Binding Energy and Nonhydrogenic Rydberg Series in Monolayer WS2. *Phys Rev Lett* **113**, (2014).

9 Ye, Z. L. *et al.* Probing excitonic dark states in single-layer tungsten disulphide. *Nature* **513**, 214-218, (2014).

10 Xiao, D., Liu, G. B., Feng, W. X., Xu, X. D. & Yao, W. Coupled Spin and Valley Physics in Monolayers of MoS2 and Other Group-VI Dichalcogenides. *Phys Rev Lett* **108**, (2012).

11 Xu, X. D., Yao, W., Xiao, D. & Heinz, T. F. Spin and pseudospins in layered transition metal dichalcogenides. *Nat Phys* **10**, 343-350, (2014).

12 Komsa, H. P. & Krasheninnikov, A. V. Electronic structures and optical properties of realistic transition metal dichalcogenide heterostructures from first principles. *Phys Rev B* **88**, (2013).

13 Gong, C. *et al.* Band alignment of two-dimensional transition metal dichalcogenides: Application in tunnel field effect transistors. *Appl Phys Lett* **103**, (2013).

14 Terrones, H., Lopez-Urias, F. & Terrones, M. Novel hetero-layered materials with tunable direct band gaps by sandwiching different metal disulfides and diselenides. *Sci Rep-Uk* **3**, (2013).

15 Stormer, H. L., Dingle, R., Gossard, A. C., Wiegmann, W. & Sturge, M. D. 2-Dimensional Electron-Gas at a Semiconductor-Semiconductor Interface. *Solid State Commun* **29**, 705-709, (1979).

16 Bellus, M. Z. *et al.* Type-I van der Waals heterostructure formed by MoS2 and ReS2 monolayers. *Nanoscale Horiz* **2**, 31-36, (2017).

17 Chiu, M. H. *et al.* Determination of band alignment in the single-layer MoS2/WSe2 heterojunction. *Nat Commun* **6**, (2015).

18 Ozcelik, V. O., Azadani, J. G., Yang, C., Koester, S. J. & Low, T. Band alignment of two-dimensional semiconductors for designing heterostructures with momentum space matching. *Phys Rev B* **94**, (2016).

19 Hong, X. P. *et al.* Ultrafast charge transfer in atomically thin MoS2/WS2 heterostructures. *Nat Nanotechnol* **9**, 682-686, (2014).

20 Wang, K. *et al.* Interlayer Coupling in Twisted WSe2/WS2 Bilayer Heterostructures Revealed by Optical Spectroscopy. *Acs Nano* **10**, 6612-6622, (2016).

21 Kozawa, D. *et al.* Evidence for Fast Interlayer Energy Transfer in MoSe2/WS2 Heterostructures. *Nano Lett* **16**, 4087-4093, (2016).

22 Zhang, C. X. *et al.* Systematic study of electronic structure and band alignment of monolayer transition metal dichalcogenides in Van der Waals heterostructures. *2d Mater* **4**, (2017).

23 Debbichi, L., Eriksson, O. & Lebegue, S. Electronic structure of two-dimensional transition metal dichalcogenide bilayers from ab initio theory. *Phys Rev B* **89**, (2014).
24 Zhang, J. F., Xie, W. Y., Zhao, J. J. & Zhang, S. B. Band alignment of two-dimensional lateral heterostructures. *2d Mater* **4**, (2017).
25 Qiu, D. Y., da Jornada, F. H. & Louie, S. G. Screening and many-body effects in two-dimensional crystals: Monolayer MoS2. *Phys Rev B* **93**, (2016).
26 Wilson, N. R. *et al.* Determination of band offsets, hybridization, and exciton binding in 2D semiconductor heterostructures. *Sci Adv* **3**, (2017).
27 Hill, H. M., Rigosi, A. F., Rim, K. T., Flynn, G. W. & Heinz, T. F. Band Alignment in MoS2/WS2 Transition Metal Dichalcogenide Heterostructures Probed by Scanning Tunneling Microscopy and Spectroscopy. *Nano Lett* **16**, 4831-4837, (2016).
28 Ceballos, F., Bellus, M. Z., Chiu, H. Y. & Zhao, H. Ultrafast Charge Separation and Indirect Exciton Formation in a MoS2-MoSe2 van der Waals Heterostructure. *Acs Nano* **8**, 12717-12724, (2014).
29 Heo, H. *et al.* Interlayer orientation-dependent light absorption and emission in monolayer semiconductor stacks. *Nat Commun* **6**, (2015).
30 Zhu, H. M. *et al.* Interfacial Charge Transfer Circumventing Momentum Mismatch at Two-Dimensional van der Waals Heterojunctions. *Nano Lett* **17**, 3591-3598, (2017).
31 Ji, Z. H. *et al.* Robust Stacking-Independent Ultrafast Charge Transfer in MoS2/WS2 Bilayers. *Acs Nano* **11**, 12020-12026, (2017).
32 Chen, H. L. *et al.* Ultrafast formation of interlayer hot excitons in atomically thin MoS2/WS2 heterostructures. *Nat Commun* **7**, (2016).
33 Ceballos, F., Ju, M. G., Lane, S. D., Zeng, X. C. & Zhao, H. Highly Efficient and Anomalous Charge Transfer in van der Waals Trilayer Semiconductors. *Nano Lett* **17**, 1623-1628, (2017).
34 Lee, C.-H. *et al.* Atomically thin p-n junctions with van der Waals heterointerfaces. *Nat Nanotechnol* **9**, 676, (2014).
35 Rigos, A. F., Hill, H. M., Li, Y. L., Chernikov, A. & Heinz, T. F. Probing Interlayer Interactions in Transition Metal Dichalcogenide Heterostructures by Optical Spectroscopy: MoS2/WS2 and MoSe2/WSe2. *Nano Lett* **15**, 5033-5038, (2015).
36 Pan, S. D., Ceballos, F., Bellus, M. Z., Zereshki, P. & Zhao, H. Ultrafast charge transfer between MoTe2 and MoS2 monolayers. *2d Mater* **4**, (2017).
37 Xu, W. G. *et al.* Correlated fluorescence blinking in two-dimensional semiconductor heterostructures. *Nature* **541**, 62-+, (2017).
38 Ceballos, F., Bellus, M. Z., Chiu, H. Y. & Zhao, H. Probing charge transfer excitons in a MoSe2-WS2 van der Waals heterostructure. *Nanoscale* **7**, 17523-17528, (2015).
39 Li, Y. Y. *et al.* Ultrafast Interlayer Electron Transfer in Incommensurate Transition Metal Dichalcogenide Homobilayers. *Nano Lett* **17**, 6661-6666, (2017).
40 Rivera, P. *et al.* Observation of long-lived interlayer excitons in monolayer MoSe2-WSe2 heterostructures. *Nat Commun* **6**, (2015).
41 Robert, C. *et al.* Exciton radiative lifetime in transition metal dichalcogenide monolayers. *Phys Rev B* **93**, (2016).
42 Xu, W. S. *et al.* Determining the Optimized Interlayer Separation Distance in Vertical Stacked 2D WS2:hBN:MoS2 Heterostructures for Exciton Energy Transfer. *Small* **14**, (2018).
43 Mak, K. F., Lee, C., Hone, J., Shan, J. & Heinz, T. F. Atomically Thin MoS2: A New Direct-Gap Semiconductor. *Phys Rev Lett* **105**, (2010).
44 Splendiani, A. *et al.* Emerging Photoluminescence in Monolayer MoS2. *Nano Lett* **10**, 1271-1275, (2010).
45 Zhu, X. Y. *et al.* Charge Transfer Excitons at van der Waals Interfaces. *J Am Chem Soc* **137**, 8313-8320, (2015).
46 Wang, H. *et al.* The role of collective motion in the ultrafast charge transfer in van der Waals heterostructures. *Nat Commun* **7**, (2016).
47 Zhang, J. *et al.* Interlayer-State-Coupling Dependent Ultrafast Charge Transfer in MoS2/WS2 Bilayers. *Adv Sci* **4**, (2017).

48 Long, R. & Prezhdo, O. V. Quantum Coherence Facilitates Efficient Charge Separation at a MoS2/MoSe2 van der Waals Junction. *Nano Lett* **16**, 1996-2003, (2016).

49 Li, L. Q., Long, R. & Prezhdo, O. V. Charge Separation and Recombination in Two-Dimensional MoS2/WS2: Time-Domain ab Initio Modeling. *Chem Mater* **29**, 2466-2473, (2017).

50 Kang, J., Li, J. B., Li, S. S., Xia, J. B. & Wang, L. W. Electronic Structural Moire Pattern Effects on MoS2/MoSe2 2D Heterostructures. *Nano Lett* **13**, 5485-5490, (2013).

51 Tong, Q. J. *et al.* Topological mosaics in moire superlattices of van der Waals heterobilayers. *Nat Phys* **13**, 356-362, (2017).

52 Wang, Y., Wang, Z., Yao, W., Liu, G. B. & Yu, H. Y. Interlayer coupling in commensurate and incommensurate bilayer structures of transition-metal dichalcogenides. *Phys Rev B* **95**, (2017).

53 Zheng, Q. J. *et al.* Phonon-Assisted Ultrafast Charge Transfer at van der Waals Heterostructure Interface. *Nano Lett* **17**, 6435-6442, (2017).

54 Jin, C. H. *et al.* On Optical Dipole Moment and Radiative Recombination Lifetime of Excitons in WSe2. *Adv Funct Mater* **27**, (2017).

55 Zhang, X. X., You, Y. M., Zhao, S. Y. F. & Heinz, T. F. Experimental Evidence for Dark Excitons in Monolayer WSe2. *Phys Rev Lett* **115**, (2015).

56 Korn, T., Heydrich, S., Hirmer, M., Schmutzler, J. & Schuller, C. Low-temperature photocarrier dynamics in monolayer MoS2. *Appl Phys Lett* **99**, (2011).

57 Amani, M. *et al.* Near-unity photoluminescence quantum yield in MoS2. *Science* **350**, 1065-1068, (2015).

58 Moody, G. *et al.* Intrinsic homogeneous linewidth and broadening mechanisms of excitons in monolayer transition metal dichalcogenides. *Nat Commun* **6**, (2015).

59 Lagarde, D. *et al.* Carrier and Polarization Dynamics in Monolayer MoS2. *Phys Rev Lett* **112**, (2014).

60 Wang, Q. S. *et al.* Valley Carrier Dynamics in Mono layer Molybdenum Disulfide from Helicity-Resolved Ultrafast Pump-Probe Spectroscopy. *Acs Nano* **7**, 11087-11093, (2013).

61 Hao, K. *et al.* Direct measurement of exciton valley coherence in monolayer WSe2. *Nat Phys* **12**, 677-+, (2016).

62 Mai, C. *et al.* Many-Body Effects in Valleytronics: Direct Measurement of Valley Lifetimes in Single-Layer MoS2. *Nano Lett* **14**, 202-206, (2014).

63 Zhu, C. R. *et al.* Exciton valley dynamics probed by Kerr rotation in WSe2 monolayers. *Phys Rev B* **90**, (2014).

64 Mak, K. F., He, K. L., Shan, J. & Heinz, T. F. Control of valley polarization in monolayer MoS2 by optical helicity. *Nat Nanotechnol* **7**, 494-498, (2012).

65 Zeng, H. L., Dai, J. F., Yao, W., Xiao, D. & Cui, X. D. Valley polarization in MoS2 monolayers by optical pumping. *Nat Nanotechnol* **7**, 490-493, (2012).

66 Cao, T. *et al.* Valley-selective circular dichroism of monolayer molybdenum disulphide. *Nat Commun* **3**, (2012).

67 Glazov, M. M. *et al.* Exciton fine structure and spin decoherence in monolayers of transition metal dichalcogenides. *Phys Rev B* **89**, (2014).

68 Yu, T. & Wu, M. W. Valley depolarization due to intervalley and intravalley electron-hole exchange interactions in monolayer MoS2. *Phys Rev B* **89**, (2014).

69 Yu, H. Y., Liu, G. B., Gong, P., Xu, X. D. & Yao, W. Dirac cones and Dirac saddle points of bright excitons in monolayer transition metal dichalcogenides. *Nat Commun* **5**, (2014).

70 Maialle, M. Z., Silva, E. A. D. E. & Sham, L. J. Exciton Spin Dynamics in Quantum-Wells. *Phys Rev B* **47**, 15776-15788, (1993).

71 Hao, K. *et al.* Trion valley coherence in monolayer semiconductors. *2d Mater* **4**, (2017).

72 Volmer, F. *et al.* Intervalley dark trion states with spin lifetimes of 150 ns in WSe2. *Phys Rev B* **95**, (2017).

73 Plechinger, G. *et al.* Trion fine structure and coupled spin-valley dynamics in monolayer tungsten disulfide. *Nat Commun* **7**, (2016).

74 Zhang, X. X. *et al.* Magnetic brightening and control of dark excitons in monolayer WSe2. *Nat Nanotechnol* **12**, 883-+, (2017).

75 Jiang, C. Y. *et al.* Microsecond dark-exciton valley polarization memory in two-dimensional heterostructures. *Nat Commun* **9**, (2018).

76 You, Y. M. *et al.* Observation of biexcitons in monolayer WSe2. *Nat Phys* **11**, 477-U138, (2015).

77 Chen, S., Goldstein, T., Taniguchi, T., Watanabe, K. & Yan, J. Coulomb-bound four- and five-particle valleytronic states in an atomically-thin semiconductor. *Arxiv*, 1802.10247, (2018).

78 Dey, P. *et al.* Gate-Controlled Spin-Valley Locking of Resident Carriers in WSe2 Monolayers. *Phys Rev Lett* **119**, (2017).

79 Song, X. L., Xie, S. E., Kang, K., Park, J. & Sih, V. Long-Lived Hole Spin/Valley Polarization Probed by Kerr Rotation in Monolayer WSe2. *Nano Lett* **16**, 5010-5014, (2016).

80 Hsu, W. T. *et al.* Optically initialized robust valley-polarized holes in monolayer WSe2. *Nat Commun* **6**, (2015).

81 Yang, L. Y. *et al.* Long-lived nanosecond spin relaxation and spin coherence of electrons in monolayer MoS2 and WS2. *Nat Phys* **11**, 830-U187, (2015).

82 Fang, H. *et al.* Strong interlayer coupling in van der Waals heterostructures built from single-layer chalcogenides. *P Natl Acad Sci USA* **111**, 6198-6202, (2014).

83 Nagler, P. *et al.* Interlayer exciton dynamics in a dichalcogenide monolayer heterostructure. *2d Mater* **4**, (2017).

84 Rivera, P. *et al.* Valley-polarized exciton dynamics in a 2D semiconductor heterostructure. *Science* **351**, 688-691, (2016).

85 Hsu, W. T. *et al.* Negative circular polarization emissions from WSe2/MoSe2 commensurate heterobilayers. *Nat Commun* **9**, (2018).

86 Hanbicki, A. T. *et al.* Double Indirect Interlayer Exciton in a MoSe2/WSe2 van der Waals Heterostructure. *Arxiv*, 1802.05310, (2018).

87 Ciarrocchi, A. *et al.* Control of interlayer excitons in two-dimensional van der Waals heterostructures. *Arxiv*, 1803.06405, (2018).

88 Yu, H. Y., Wang, Y., Tong, Q. J., Xu, X. D. & Yao, W. Anomalous Light Cones and Valley Optical Selection Rules of Interlayer Excitons in Twisted Heterobilayers. *Phys Rev Lett* **115**, (2015).

89 Yu, H. Y., Liu, B. L. & Yao, W. Brightened spin-triplet interlayer excitons and optical selection rules in van der Waals heterobilayers. 1803.01292, (2018).

90 Miller, B. *et al.* Long-Lived Direct and Indirect Interlayer Excitons in van der Waals Heterostructures. *Nano Lett* **17**, 5229-5237, (2017).

91 Kunstmann, J. *et al.* Momentum-space indirect interlayer excitons in transition-metal dichalcogenide van der Waals heterostructures. *Nat Phys*, (2018).

92 Wu, F. C., Lovorn, T. & MacDonald, A. H. Theory of optical absorption by interlayer excitons in transition metal dichalcogenide heterobilayers. *Phys Rev B* **97**, (2018).

93 Yu, H. Y., Liu, G. B., Tang, J. J., Xu, X. D. & Yao, W. Moire excitons: From programmable quantum emitter arrays to spin-orbit-coupled artificial lattices. *Sci Adv* **3**, (2017).

i94 Kim, J. *et al.* Observation of ultralong valley lifetime in WSe2/MoS2 heterostructures. *Sci Adv* **3**, (2017).

95 Jin, C. H. *et al.* Imaging of Pure Spin-Valley Diffusion Current in WS2/WSe2 Heterostructures. *Science*, in press, (2018).

96 Carvalho, B. R. *et al.* Intervalley scattering by acoustic phonons in two-dimensional MoS2 revealed by double-resonance Raman spectroscopy. *Nat Commun* **8**, (2017).

97 Hill, H. M. *et al.* Observation of Excitonic Rydberg States in Monolayer MoS2 and WS2 by Photoluminescence Excitation Spectroscopy. *Nano Lett* **15**, 2992-2997, (2015).

98 He, K. L. *et al.* Tightly Bound Excitons in Monolayer WSe2. *Phys Rev Lett* **113**, (2014).

Acknowledgements

E.Y.M. acknowledge support from the Department of Energy, Office of Science, Basic Energy Sciences, Materials Sciences and Engineering Division, under Contract DE-AC02-76SF00515; T. F.H. acknowledges support from the AMOS program, Chemical Sciences, Geosciences, and Biosciences Division, Basic Energy Sciences, US Department of Energy under Contract DE-AC02-76-SF00515 and from the Betty and Gordon Moore Foundation's EPiQS Initiative through Grant No. GBMF4545. O.K. acknowledges the support of the Rothschild Fellowship of Yad Hanadiv Fund, Israel, and of the Viterbi Fellowship of the Andrew and Erna Viterbi Department of Electrical Engineering, Technion, Israel. F.W. and E.C.R. acknowledge support from the Director, Office of Science, Office of Basic Energy Sciences, Materials Sciences and Engineering Division of the U.S. Department of Energy under Contract No. DE-AC02-05-CH11231 (van der Waals heterostructures program, KCWF16). C.J. acknowledges the support from the National Science Foundation EFRI program (EFMA-1542741).